Title	Antifouling coatings made with Cold Spray onto polymers: Process characterization
Authors(s)	Lupoi, R.; Stenson, C.; McDonnell, Kevin; Dowling, Denis P.; Ahearne, Eamonn
Publication date	2016
Publication information	CIRP Annals - Manufacturing Technology, 65 (1): 545-548
Publisher	Elsevier
Item record/more information	http://hdl.handle.net/10197/7998
Publisher's statement	þÿ This is the author s version of a work that was accepted for Manufacturing Technology. Changes resulting from the publishing process, such as peer review, editing, corrections, structural formatting, and other quality control mechanisms may not be reflected in this document. Changes may have been made to this work since it was submitted for publication. A definitive version was subsequently published in CIRP Annals - Manufacturing Technology (65, 1, (2016)) DOI:10.1016/j.cirp.2016.04.015
Publisher's version (DOI)	10.1016/j.cirp.2016.04.015

Functionalizing polymer surfaces with Cold Spray for applications in bioenvironments

R. Lupoi[a], C. Stenson[a], K. A. McDonnell[b], D.P. Dowling[b], E. Ahearne (2)[b]

[a]Trinity College Dublin, The University of Dublin, Department of Mechanical and Manufacturing Engineering, Parsons Building, Dublin 2, Ireland.
[b]University College Dublin, School of Mechanical and Materials Engineering, Belfield, Dublin 4, Ireland.

Cold Spray (CS) of copper particles onto polymers has been validated as an effective tool for maintaining surface integrity in bioenvironments. CS requires limited heat input, can be applied locally or in large areas. The key parameters are particle penetration depth and copper surface coverage. However, the process parameters that can optimize the coating performance with deposition have not been comprehensively explored. In this paper, copper particles were deposited onto two polymers used in marine applications. A detailed analysis was carried out to correlate the key surface properties to the process so as to determine the optimum conditions.

Coating; Processing; Cold Spray

1. Introduction

Biofouling is a critical problem that occurs when a solid structure is in contact with a bioenvironment, specifically in water. Attachment of foulers increases hydrodynamic drag and adds weight to vessels affecting fuel efficiency. Consumption can increase by as much as 40% while maximum speed is reduced [1]. Aquaculture nets, meshes and flotation devices are also victims. Increased weight and drag on nets, cages and flotation devices causes unpredictable behaviour in rough seas and cleaning is costly [2].

The typical approach to prevent fouling is to use coatings containing biocides. Modern antifouling (AF) paints contain copper which is an effective biocide in surface boundary layers. This method is compatible with most metallic, wooden and polymer structures to which paint can be easily applied. However, due to their inherently low surface energy thermoplastic polymers are difficult to paint or coat [3]. This represents a potential barrier to their use for marine applications.

Recent studies have demonstrated the potential to functionalise polymeric materials using Cold Spray (CS). Shallow embedment (<100µm) of metal particles beneath the surface of thermoplastics can improve surface performance. Copper impregnation gave AF capability which prevented attachment for upwards of 250 days [4]. The primary factors controlling AF efficacy are particle coverage – as well as the depth of embedment [5].

In its typical form, CS is a manufacturing process that uses a carrier gas (such as nitrogen or helium) to accelerate particles up to supersonic speed within a converging-diverging nozzle. Once the particles reach a minimum velocity upon impact against a surface they deform sufficiently to create a dense coating. The process is currently used for a number of applications, including the deposition of stellite materials to enhance wear resistance in steel moulds [6]. Below the minimum velocity the particles either cause erosion of the substrate or bounce off without noticeable damage [7]. Specifically, particle embedment to produce AF functionality requires particle velocities in the transition region between erosion and coating formation [8].

The studies of particle embedment with CS for AF carried out to date have used carrier gas pre-heating, giving higher particle speed at the nozzle exit, to achieve the required coverage and embedment depth. Gas heating increases gas and by extension particle velocity and is reported to cause softening of thermoplastic polymers. This leads to increased penetration, facilitating a larger amount of AF material embedment per unit area [8]. However, the use of heating presents a problem in terms of applicability of the process at the industrial level. Hot gases exiting the nozzle lead to thermal distortion of polymer surfaces generating irrecoverable changes in geometry. In this paper, we have investigated the use of cold processing parameters instead. Utilizing a high velocity nozzle design that does not require gas heating to achieve the threshold particle velocity, copper was embedded in two thermoplastic polymers commonly used in marine environments. Surfaces were analysed to determine the degree of deposition and surface coverage in order to compare with deposits made for AF purposes reported in the literature but achieved with gas heating. Roughness was investigated as a link to understand the effect of the process on hydrodynamic performance. Different spray parameters were also varied so that optimum conditions could be identified.

2. Experimental Procedure

Two different polymer materials were used in the investigation. Sheets of high density polyethylene (HDPE) and polytetrafluoroethylene (PTFE) measuring 3mm thick were cut into roughly 150 x 200 mm square sections for spraying. HDPE is a thermoplastic polymer commonly used in aquaculture pens and boat hulls and PTFE is often used in heat exchangers for aquaculture [9]. The critical parameters for an efficient AF coating are surface density and particle penetration depth; the experimental study was therefore focused at the quantification of those. An in-house CS facility (in Trinity Collge Dublin) was used for the trials. It consists of a two-axis CNC X-Y table with the CS nozzle manoeuvrable in the Z direction. Unheated, pressurised nitrogen was used as the carrier gas which was drawn from external bottles through a regulator. The powder feeder was a high-pressure commercial unit (Uniquecoat - PF100WL). It allows changes in particle feed-rate by selecting the speed of an internal wheel, expressed in % of the maximum rotational velocity. The nozzle used was a stainless steel De-Laval type (in-house design) with throat diameter of 2mm and exit diameter 6mm. Converging and diverging lengths were 30mm and 180mm respectively and the stand-off-distance was set to 40mm. Static pressure of the gas was monitored at the nozzle inlet and values quoted will refer to
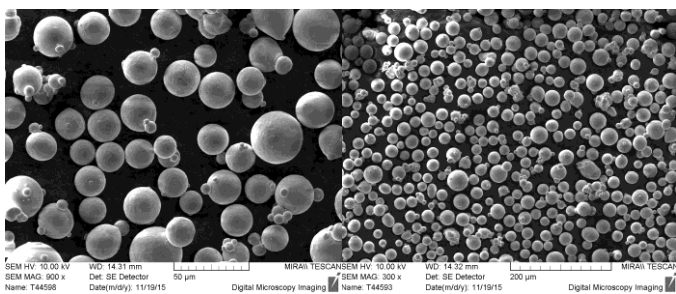
Figure 1. SEM images of copper powder before spraying.

this pressure. The copper powder used was 99.95% pure by atomic weight, and is characterized by spherical geometry. The nominal size of the powder was between 15μm and 38μm. Figure 1 shows an SEM image of the feedstock material. Static pressure, particle feed rate and nozzle scan speed (or transverse speed) were varied in order to evaluate the optimum parameters so as to achieve AF protection under cold processing conditions.

The particle penetration depth was measured from the polymer surface down to the deepest point of the coating by looking at images of the coating cross section with an optical microscope. Particles depths were measured in five random images for each sample and the mean depth was calculated. The surface coverage was visually calculated with a software (ImageJ V1.50) using the row images taken with the optical microscope at the coating surface. This was carried out for five images of each sample and the mean surface coverage was calculated. The techniques mentioned above for calculating surface coverage and penetration depth are aligned with reported procedures in literature [4].

The Shore D Hardness of the polymers before being sprayed was measured using a Shore durometer. Measurements were obtained by applying a continuous force to the top of the durometer until the indenter was fully embedded in the polymer. The maximum reading was used. Five measurements were taken for each material and the mean value calculated. The morphology and surface roughness of the sample surfaces was examined using a Wyko NT110 optical Profilometer operating in Vertical Scanning Interferometry (VSI) mode at a magnification of 25 x. Five measurements per sample were taken at randomly selected points. Roughness measurements are quoted in Ra. In order to obtain data on the kinetic energy of the particles upon impact with the substrate, Computational Fluid Dynamics (CFD) simulations of the nozzle were carried out using ANSYS Fluent 16.0. A 2D axial-symmetric geometry was constructed and a mesh created using the ANSYS meshing tool. The total number of grid elements was 86,100 to provide a grid-independent solution. The High-Mach-Number drag law was used to model drag on the particles along with a realizable k-ε turbulence model with non-equilibrium wall functions. Particle shape was assumed spherical and diameter constant for the simulations. The median of the nominal particle range size – 26.5μm – was used as the particle diameter in the simulations. Using a second order discretization scheme the solutions were iterated until convergence was reached. The resulting particle velocity values from the CFD were used to calculate the kinetic energy of the particles on impact according to $E = 1/2mv^2$, where "E" is the impact energy, "m" is the particle mass and "v" is the particle velocity at the substrate impact location. Particle mass was calculated by taking density of copper as 8960 kg/m^3 and assuming the same particle diameter as in the CFD simulations. CFD was therefore used to predict the particle velocity, and the corresponding energy, at impact against the substrate.

3. Results and Discussion

3.1. Penetration Depth

Figure 2 shows the penetration depth results for HDPE and PTFE. Penetration depth was graphed against particle impact energy which is a function of the nozzle inlet pressure. The overall trends are rather similar, however with some differences that could be attributed to the hardness levels (the measured hardnesses were 60.4 and 65.2 Shore D for PTFE and HDPE respectively). In both cases we see an overall trend of enhanced penetration depth with increasing particle impact energy. There were exceptions, notably at the highest impact energy with each material. At this point the onset of severe erosion resulted in lower penetration. Surface erosion had been negligible prior to this point in the HDPE, but became observable in the PTFE as early as from second lowest
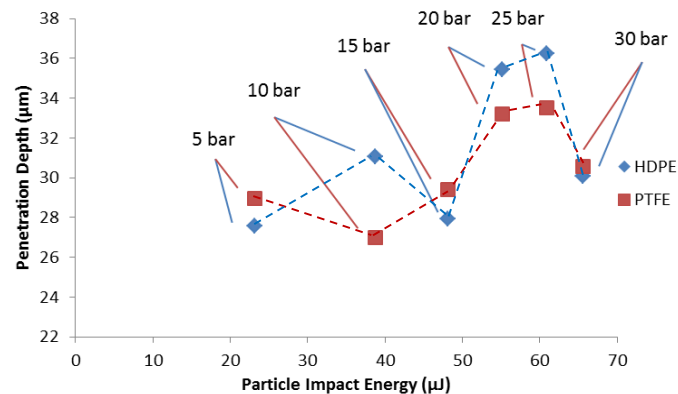

Figure 2. Penetration depth results for HDPE and PTFE (scan speed = 50mm/s; powder feeder wheel speed = 30%)

impact energy. It is in fact clear that due to erosion the overall values of particle penetration were lower for the PTFE (the softer material) substrate, as opposed to HDPE. The highest particle penetration achieved was at impact energies between 55 and 61 μJ.

In order to understand the effect of process speed and particle feed rate on penetration depth, experiments were carried out (at 15 bar inlet pressure) when varying the nozzle scan speed and
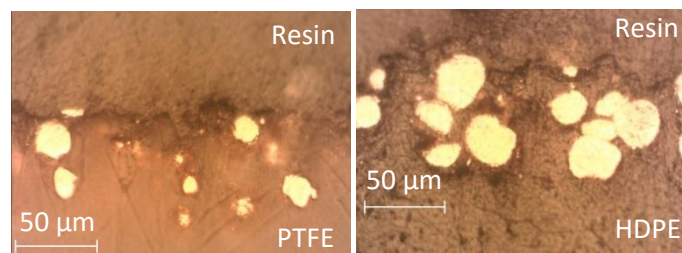

Figure 3. Cross section at 48 μJ impact energy, 100 mm/s scan speed and 45% wheel speed

Figure 4. CS at 48 μJ impact energy 25 mm/s scan speed and 35% wheel speed.

feeder wheel velocity within the 25-100mm/s and 30-60% range respectively. 15 bar was chosen as it was judged to result in the best balance between achieving deposition and avoiding erosion following a visual inspection at the time of the experiments. It was observed that increasing the particle feed rate and reducing the nozzle scan speed can result in a small increment of penetration depth. However, the most critical role is clearly played by the achievable impact energy, i.e. particle velocity at the surface. Figure 3 and Figure 4 show examples of obtained coating cross-sections. It is clear that the deposition mode allows for multiple particle layers impregnated below the surface of the polymers, suggesting the deposited layer is actually well consolidated within the softer matrix.

3.2. Surface Coverage

Figure 5 shows the surface coverage results obtained for HDPE. A clear trend of increasing surface coverage with increasing particle impact energy is observed also in this case. The highest surface coverage (64%) occurred at 55μJ impact energy. This
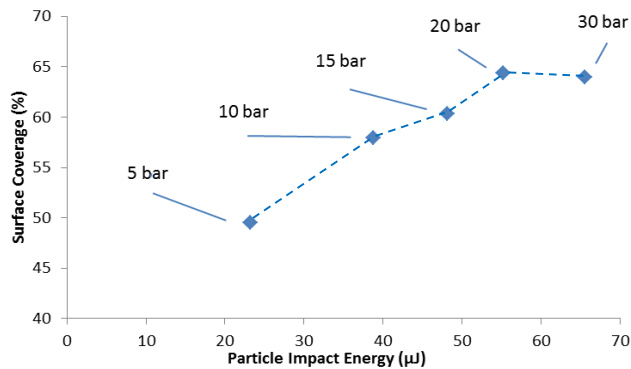

Figure 5. Surface coverage measurements for HDPE. Scan speed = 50mm/s; wheel speed = 30%.

also corresponds to one of the highest embedment depths from Figure 2. Also in this case, the best coverage is therefore achieved at the highest particle impact energy. Changing the nozzle scan speed and the powder feeder wheel velocity did not produce any
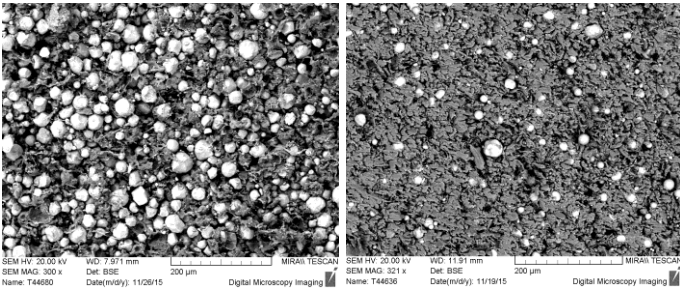

Figure 6. SEM surface images at 48 μJ impact energies for HDPE (a) and PTFE (b).

notable improvement to what is reported in Figure 5. Figure 6 shows SEM images at the surface for the two polymers; the presence of copper particles can be clearly observed. It can also be noticed that difficulty was encountered towards the achievement of a high surface coverage on PTFE, and in this respect the two deposition modes are evident in the close-up images in Figure 7. In the case of HDPE the polymer matrix, despite being bombarded at the surface, is able to maintain a continuous structure capable of holding the particles firmly. It is also evident that some particles have "bounced off" and left an empty crater on the surface. The post-processed surface morphology in the PTFE case appears totally different. The particle bombardment has in fact caused shredding of the surface, hence less suitable conditions for a high degree of particle impregnation. Thresholding of PTFE was harder as the polymer colour is similar to the copper in the images; however the surface coverage did not exceed 15% and was not included in Figure 5.
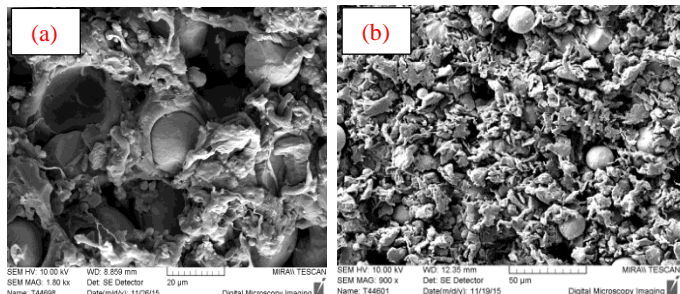

Figure 7. SEM surface images (a) for HDPE and (b) for PTFE.

Observations from Figure 6 and 7 therefore suggest PTFE can be less suitable for particles impregnation with CS, as it was not possible to achieve satisfactory levels of surface coverage over the outer layer. In Figure 3 it can be noticed that, despite a good penetration depth, less copper is overall impregnated in the matrix.

3.3. Surface Roughness

In applications in which AF protection is required the issue of hydrodynamic drag can be important. It has already been mentioned that the increase in skin friction caused by fouling decreases efficiency of vessels and contributes to unpredictable behaviour in aquaculture equipment. CS is a surface modification technique which will ultimately affect the surface roughness. This has therefore been measured to further understand the impact of variable processing parameters.
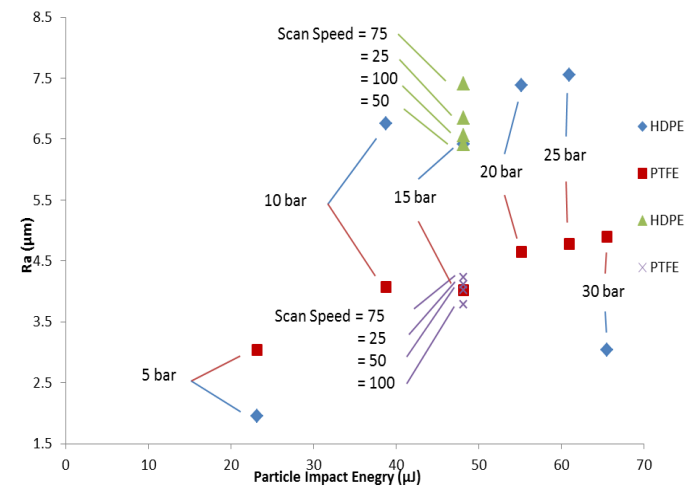

Figure 8. Surface roughness measurements after spraying (Scan speed = 50mm/s and wheel speed = 30% unless otherwise indicated).

Figure 8 shows the measured values of surface roughness using the cold spray parameters explored. It is clear from the representation that levels are much higher for HDPE than PTFE in almost all cases. This is due to the greater copper surface area coverage evident on HDPE leading to more surface roughening, and discussed in the previous section. The highest roughness values occurred for impact energies of 55 and 61μJ for HDPE and 55, 61 and 66μJ for PTFE. Given that these were the impact energies at which the highest surface coverage and penetration depths also occurred, it appears that the parameters required to provide the best penetration depth and surface coverage also lead to the greatest surface roughness. In this case the data generated at different nozzle scan speeds (at 15 bar) are also included as they had a measurable effect. In this respect, results did not show a clear trend distribution, with the maximum Ra measured at 75mm/s in both cases. On average, moving the nozzle faster led to lower Ra levels. Powder feeder wheel speed, i.e. particle feed rate, had a negligible effect on surface roughness measurements for both materials.

3.4 Process window and performance prediction

Figure 9 shows a process chart summarising the effects of the parameters which were explored for embedment into HDPE. It is intended to guide possible users towards the employment of the correct spray conditions, at least from an initial perspective and with equipment similar to what was used in this study. Results for the PTFE case are not being included in the chart as the copper impregnation was demonstrated not to be as efficient.

The findings show that particle impact energies in the region of 23μJ, achieved using low gas pressure, resulted in poor surface coverage as well as limited penetration depth. Higher pressures, leading to greater impact energies, were required for larger embedment depths and also provided large surface coverage. However, care must be taken when increasing impact energy not

applicability to a restricted materials range. The coatings were achieved with a high-speed nozzle using nitrogen carrier gas but without gas-heating for the first time; hence the disadvantages of heat exposure on the polymer surfaces were eliminated. The effects of various process parameters were graphically represented in a processing chart. This illustrates the areas of low
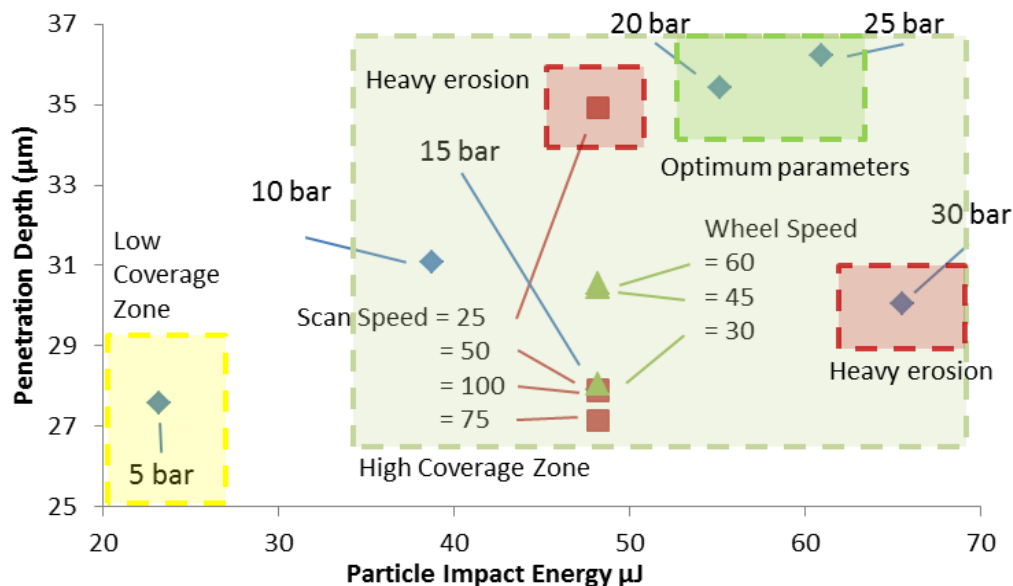

Figure 9. Process summary chart for HDPE.

to enter into the deposition through erosion window. As well as causing loss of material, erosion also led to reduced penetration depth. This occurred at an impact energy of 66μJ. Erosion can also occur at lower energy levels when reducing the nozzle scan speed. The optimum parameters identified in this study were at impact energies within the 55 to 61μJ range with a nozzle scan speed of 50 mm/s and powder feeder wheel speed of 30%. These gave high embedment depths of around 35 μm and good surface coverage of 57 – 60% without observable surface erosion. Figure 9 includes the identification of initial "zones" showing the transition boundaries between different regimes. However, in order to identify more precisely each zone size, a more comprehensive study will be required.

AF tests carried out on CS coatings and reported in literature can provide an initial estimation on the actual performance. In [4] copper embedded into nylon with a depth of 40μm and a surface coverage of 60% provided AF protection for approximately 181 days. Comparing to other tests [10] in which only surface coverage was reported, a 12 weeks AF protection is potentially generated by the coatings produced in this study. By a way of comparison, soluble matrix paints used on boat hulls last for 12-15 months at the most. However these are not often used in aquaculture equipment given the difficulty in their application. Studies carried out on the AF protection of copper containing waxy emulsions used on aquaculture nets showed the occurrence of fouling after 150 days [11], in line with the expected performance of the coatings produced and reported in this paper.

4. Conclusion

Copper was successfully deposited on two polymers used in marine applications to provide AF protection. The embedment depth and surface coverage in HDPE were quantified and found to provide protection for a similar length of time to modern waxy emulsions used on aquaculture nets, and to other CS studies with gas heating. It was not possible to achieve good surface coverage on the PTFE material, suggesting limitations of the process

and high coverage as well as showing erosion zones and identifying the optimum parameters. This study has therefore demonstrated that AF performance can potentially be achieved with CS using optimised high speed nozzles and no gas heating; an optimum parameters window was identified to provide the best performance was identified.

References
[1] Omae, I., 2003, Organotin antifouling paints and their alternatives, Applied Organometallic Chemistry, 17/2:81-105.
[2] Greene, J.K., Grizzle, R.E., 2007, Successional development of fouling communities on open ocean aquaculture fish cages in the western Gulf of Maine, USA, Aquaculture, 262/2-4:289-301.
[3] Zuyev, K.S., Chen, X., Cabrera-Rios, M., Castro, J.M., 2001, In Mold functional coatings of thermoplastic substrates: Process Modeling, Journal of Injection Molding Technology, 5/2:80.
[4] Vucko, M.J., King, P.C., Poole, A.J., Carl, C. Jahedi, M.Z., de Nys, R., 2012 Cold spray metal embedment: an innovative antifouling technology, Biofouling, 28/3:239-248.
[5] Vucko, M.J., King, P.C., Poole, A.J., Jahedi, M.Z., de Nys, R., 2013, Polyurethane seismic streamer skins: an application of cold spray metal embedment, Biofouling, 29/1:1-9.
[6] Luchetta, G., Giusti, R., Vezzu, S., Bariani, P.F., 2015, Investigation and characterisation of Stellite-based wear-resistant coatings applied to steel moulds by cold spray, Annals of the CIRP, 64/1:535-538.
[7] Lupoi. R., O'Neill, W., 2010, Deposition of metallic coatings on polymer surfaces using cold spray, Surface and Coatings Technology, 205/7:2167-2173.
[8] King, P.C., Poole, A.J., Horne, S., de Nys, R., Gulizia, S., Jahedi, M.Z., 2013, Embedment of copper particles into polymers by cold spray, Surface Coatings Technology, 216:60-67.
[9] Fredriksson, D.W., DeCew, J.C., Tsukrov, I., 2007, Development of structural modelling techniques for evaluating plastic net pens used in marine aquaculture, Ocean Engineering, 34:2124-2137.
[10] Vucko, M.J., King, P.C., Poole, A.J., Hu, Y., Jahedi, M.Z., de Nys, R., 2014, Assessing the antifouling properties of cold-spray metal embedment using loading density gradients of metal particles, Biofouling, 29/1:1-9
[11] Braithwaite, R.A., Carrascosa, M.C.C, Mc. Evoy, L. A., 2007, Biofouling of salmon cage netting and the efficacy of a typical copper based antifoulant, Aquaculture, 262: 219-226.